Saudi Journal of Biological Sciences 28 (2021) 495–503

Contents lists available at ScienceDirect

Saudi Journal of Biological Sciences

journal homepage: www.sciencedirect.com

Original article

Green synthesis of silver nanoparticles by *Rivina humilis* leaf extract to tackle growth of *Brucella* species and other perilous pathogens

Sri Raghava, Kenneth Munnene Mbae, S. Umesha *

Department of Studies in Biotechnology, University of Mysore, Manasagangotri, Mysore 570006, Karnataka, India

ARTICLE INFO

Article history:
Received 8 August 2020
Revised 6 October 2020
Accepted 19 October 2020
Available online 28 October 2020

Keywords:
Silver nanoparticles
Rivina humilis
Characterization
Brucellosis
Biocompatibility

ABSTRACT

Novel approaches are obligatory to treat chronic intracellular bacterial infectious diseases like Brucellosis specifically, are very complicated to deal with. The aim of the study to take upon nanotechnology approach to exploit the efficacy of the synthesized nanoparticles, to overcome barriers for treatment of *Brucella* species and other pathogens. Present study used *Rivina humilis* extract as reductant of silver ions for synthesis of silver nanoparticles for the first time. Rh-AgNP's was characterized by UV–visible spectroscopy, DLS, FT-IR, SEM, EDS, TEM and XRD. Radical scavenging, antibrucellosis, bactericidal activity was evaluated. Clinical application was assessed by Rate of haemolysis, fibrinolytic and Hemagglutination activity. UV–visible spectrum of synthesized Rh-AgNP's showed maximum peak at 440 nm indicating the formation of nanoparticles. TEM showed that the average particle size of nanoparticles 51 nm with spherical shape, DLS depicted monodisperse state in water; EDS confirmed the presence of silver metal. Rh-AgNP's exhibited potential antibrucellosis activity against *B. abortus, B. melitensis* and *B. suis* effective inhibition at 800 µg/mL. The bio-compatibility of Rh-AgNP's was established by rate of haemolysis, hemagglutination and fibrinolytic activity. For the first time it has been proved that Rh-AgNP's have efficacy as antimicrobial agent with potential application in the biological domain.

1. Introduction

Brucellosis is a neglected remerging bacterial zoonotic infectious disease, that distresses domesticated animals, wild animals and humans. The overall occurrence of human brucellosis is estimated to go beyond 800,000 cases annually, of which 40% leading to chronic infection (Kirk et al., 2015). Preferred treatment specified for human brucellosis caused by *Brucella melitensis* field strains is a combination of antibiotics (Grilló et al., 2006). However, due to emerging resistance there is high rate of disease relapse and treatment failure, the major concern for the treatment of Brucellosis is that the disease is pathognomonic (Raghava et al., 2017). Thus, new approach is becoming obligatory for brucellosis treatment.

Nanotechnology advancement is promising approach leading to varied scope of applications, has a great potential to deliver the therapeutic agents to the target in the medical treatments (Vilchis-Nestor et al., 2008). Nanotechnology is the method of alteration /assembly of the atoms and molecules in which the resulted structures and material leads to different and novel properties (Hamedi et al., 2017; Pishahang et al., 2018). Lately, the progress of efficient green chemistry methods like plant based synthesis of nanoparticles has received more consideration as a substitute approach to synthesize the metal nanoparticles by minimizing the toxic and hazardous waste materials by establishing sustainability (Selvan et al., 2018; Soshnikova et al., 2018). Medicinal plants have always been vital sources for new drug discovery has they readily synthesize substances themselves to defend/ inhibit against herbivores and microorganisms (Aboaba et al., 2006). World's 80% population mainly relies on phytoproducts for health care and also for the clinically required drug sources (Werka et al., 2007). Hence in our study we applied nanotechnology for the synthesis of potential nanoparticles by using plant source *Rivina humilis*. *R. humilis* belongs to family phytocaccaceae is popularly known as pigeon berry grows well in tropical America and Africa and now widely naturalized in indo-malaysia and pacific islands. Seeds are

* Corresponding author.
E-mail address: su@appbot.uni-mysore.ac.in (S. Umesha).

Peer review under responsibility of King Saud University.

Production and hosting by Elsevier

https://doi.org/10.1016/j.sjbs.2020.10.034
1319-562X/

propagated through dispersal by birds (Tseng et al., 2008; Harsha et al., 2012). Even though many researchers have synthesized silver nanoparticles using plants very scarce have shown antibrucellosis activity. In the present study, Rh-AgNP's were synthesized, were further characterized using different analytical instruments. In addition, the antioxidant efficacy and biocompatibility was assessed by rate of haemolysis, haemagglutination and fibrinolytic activity.

2. Materials and methods

2.1. Bacterial reference strains

Brucella strains were procured from IVRI, Uttar Pradesh, India. Other bacterial strains were obtained from MTCC, Chandigarh, India and ATCC. *Staphylococcus aureus* (96), *Escherichia coli* (1610), *Bacillus cereus* (430), *Shigella flexneri* (1457), *Bacillus subtilis* (6939) and *Enterobacter aerogenes* (13048) strains.

2.2. Preparation of the plant extracts

The plant *Rivina humilis* was collected from the Western Ghats of Karnataka, India and identified by the former Dr. G. R. Shivamurthy, Professor, Department of Botany, University of Mysore, Mysuru, India (Fig. 1). Leaves were shade dried for about twenty days and ground into fine powder. Fifty grams of finely powdered *R. humilis* material was used to get the aqueous extract in 500 mL and were filtered with Whatman No.1 filter paper and collected in collection tubes and refrigerated.

2.3. Synthesis of silver nanoparticles

Ten ml of leaf plant aqueous extract was added to 90 mL of freshly prepared 1 mM silver nitrate solution ($AgNO_3$). The mixture was kept under direct sunlight the gradual colour change was noted as an indication of Rivina humilis silver nanoparticle (Rh-AgNPs) formation (Brahmachari et al., 2014; Rastogi, and Arunachalam, 2011)

Fig. 1. Plant material Rivina humilis collected from Western Ghats region of Karnataka, India.

2.4. Characterization of Rh-AgNP's

2.4.1. UV–Visible Spectroscopy

Absorption wavelength range of nanoparticles was confirmed using spectrophotometer (Hitachi U 3000, Japan). Exactly, 1 mL of the diluted supernatant of the synthesized nanoparticles were placed in a quartz cuvette with a 1 cm path length and inserted in a UV–Vis spectrophotometer to obtain the UV–Visible spectra of the sample in the 300–800 nm wavelength range against water as the reference. The surface Plasmon resonance of Rh-AgNP's was observed.

2.4.2. Dynamic light scattering (DLS) and zeta potential

The Nanotrac wave (USA) particle size analyzer was used to evaluate the particle size distribution and stability of Rh-AgNP's. The analyser gives the size measurement of the synthesized particle, the state of aggregation and zeta potential value of the synthesized Rh-AgNP's.

2.4.3. Fourier Transform Infrared Spectroscopy (FT IR)

The functional groups on the Rh-AgNP's were studied by the FT-IR analysis. The Rh-AgNP's synthesized were analysed by Bruker, Massachusetts, (USA) to reveal the distribution of biological macromolecules at spectrum ranging from wave number 400 to 4000 cm^{-1}. The number of scans and spectral resolution were set to 24 and 4 cm − 1, respectively.

2.4.4. Scanning electron microscopy (SEM) of Rh-AgNP's and Energy Dispersive X-ray Spectroscopy (EDS) of Rh-AgNP's

A drop of biosynthesized Rh-AgNP's was placed on a carbon-coated copper and allowed to air dry. After drying the image captured using HITACHI (S-3400 N, Japan) at 10 kV acceleration voltages. The Energy Dispersive X-ray Spectroscopy (EDS) analysis was carried out using HITACHI (Noran System 7, USA) system attached to SEM for the detection of elements on the sample in the AgNPs.

2.4.5. Transmission electron microscopic (TEM) for Rh-AgNP's

For morphological analysis of Rh-AgNP's, transmission electron microscopy (TEM) was performed. A drop of AgNPs solution was placed on a copper grid coated by an amorphous carbon film and dried under vacuum for further observation. More characteristics of the AgNP's including their morphology and size were identified using a high-resolution transmission electron microscope (JEM-1230, Tokyo, Japan) at an accelerating voltage of 100.0 kV.

2.4.6. X ray diffraction (XRD) analysis

The dry powder of the silver nanoparticles was analyzed by XRD. The diffracted intensities were recorded from 20 to 80° at 2 theta angles by using X-ray diffractometer XRD-6000 (shimadzu, Rigaku Corporation, Tokyo, Japan). The obtained peaks were compared with the standards. The size of the particle was calculated using the Scherer's formula.

2.5. DPPH radical scavenging activity

The radical scavenging activity of the synthesized nanoparticles was estimated using the stable DPPH radical scavenging assay described by Odeyemi et al. (2015) with slight modifications. DPPH solution was mixed with synthesized Rh-AgNP's (different concentration) and incubated for 30 min. The absorbance was measured at 517 nm. The scavenging percentage of DPPH was calculated using the formula

$$RSA(\%) = 100 \times 1 - A(S)/A(C)$$

Where, AS- absorption of the test sample and AC: DPPH solution absorbance without the test sample. All the experiments were carried out in triplicates and repeated twice.

2.6. In vitro antimicrobial efficacy of Rh-AgNP's against Brucella species

The bacterial strains were subjected to disc diffusion method according to Ghanwate et al., 2016 with slight modifications to deduce the Rh-AgNP's susceptibility. Antimicrobial study was carried out with the reference bacterial strains obtained from Indian Veterinary Research Institute, Izatnagar, India. The *Brucella* culture suspension was prepared and $1x10^6$ CFU/mL cells was inoculated on to Muller Hilton agar supplemented with 1% sheep's blood, then sterile disc (6 mm) was loaded 5 μL of different serial dilutions of Rh-AgNP's (25, 50, 100, 200, 400 and 800 μg/mL). The plates were incubated at 37 °C under 7%– 10% CO_2 for 72 h. The zone of growth inhibition was measured (Ghaderkhani et al., 2019). The test was performed in triplicates and repeated thrice.

2.7. Bactericidal effect of Rh- AgNPs on other perilous pathogen

Disc diffusion method was carried out according to Manukumar et al. (2017) with slight modifications to check the Rh-AgNP's efficacy to inhibit the growth of perilous pathogens. Gram positive *S. aureus*, *B. cereus*, *B. subtilis* and Gram negative *E. aerogenes*, *E. coli*, *S. flexneri* pathogens. The bacterial suspension was prepared from the overnight culture and $1x10^6$ CFU/mL cells inoculated on to nutrient agar, then sterile disc (6 mm) was loaded with 5 μL of different serial dilutions of Rh-AgNP's (25, 50, 100, 200, 400, 800 and 1200 μg/mL). Sterile distilled water and Streptomycin (10 μg) served as negative and positive control, respectively. The plates were sealed and incubated at 37 °C for 24 h to examine zone of inhibition. Assay was performed in triplicates and repeated thrice.

2.8. Biocompatibility assay

2.8.1. Rate of haemolysis

Different concentrations (1, 5, 10, 20, 40, 80, 100, 200 400, 800 and 1200 μg/mL^{-1}) of Rh-AgNP's and freshly collected human blood was mixed and incubated at 37 °C for 30 min. Centrifuged, supernatant was collected and absorbance was measured at 545 nm (Manukumar et al., 2017; Huang et al., 2016). Assay was performed in triplicates and repeated thrice. Haemolysis rate was determined by:

$$HR = OD\ treated - OD\ negative\ control \times 100/OD\ positive\ control - OD\ negative\ control$$

2.8.2. Fibrinolytic activity

Citrated sheep plasma 100 μL and 0.25 M $CaCl_2$ 30 μL was mixed to form a soft clot fibrin at 37 °C for 3 h, then washed, resuspended with PBS (pH 7.4) and mixed with 500 μL Rh-AgNP's in Tris-HCl buffer (pH 8.5) incubated for 2 h at 37 °C. Finally, 750 μL of 0.44 M TCA was added to cause the precipitation of the undigested clot according to protocol of Harish et al. (2015) Centrifuged and protein content in the supernatant was determined using Folin-Ciocaltues reagent to know the fibrinolytic activity.

2.8.3. Hemagglutination assay

100 μL Phosphate Buffer Saline of pH 7.4 and 100 μL Rh-AgNP's were added into microtiter plate and mixed different concentration from 1 to 1200 μg/mL were added till column 12. Then 100 μL of red blood cells was added to each well and incubated at room temperature for 30–60 min (Amruthraj et al., 2015).

2.9. Statistical analysis

ORIGIN, SPSS software (version 15) used for statistical analysis and T-test to compare the groups. P-value of < 0.05 was considered significant. All the tests were done in triplicates and repeated thrice.

3. Results and discussion

3.1. Synthesis of Rh-AgNP's

Synthesis of Rh-AgNP's arising from reduction of $AgNO_3$ by constituents of *Rivina humilis* leaf aqueous extract was indicated by an observable change in colour to a reddish brown Similar observations have been presented by other investigators using plant extracts as sources of reductants of ionic silver into nanoparticles. Upon exposure of *Ocimum sanctum* extract and silver nitrate solution in the sunlight, a dark brown-reddish colour mixture was witnessed (Brahmachari et al., 2014). Use of *P. longum* by the Jayapriya et al., (2019) adduced similar observation.

3.2. Characterization of nanoparticles

3.2.1. UV–visible spectroscopy

Plasmonic metallic nanoparticles possess fascinating optical properties. Therefore, 300–800 nm UV–visible spectroscopy range can be used to gather useful information about metal nanoparticles within 2 to 100 nm dimensions' interval (Singh et al., 2016). Typical of Ag-NPs having λ_{max} values in the visible range of 440 – 460 nm (Thangaraju et al., 2012; Manukumar et al., 2017; Muthuraman et al., 2019). The position of a Surface Plasmon Resonance (SPR) peak arising from oscillation of conduction band electrons has a bearing on the nature, shape and size of AgNPs (Bastús et al., 2015). The SPR peak for Rh-AgNP's was located 440 nm (Fig. 2).

3.2.2. DLS and zeta potential

Dynamic light scattering size analysis gave an average particle diameter of 51 nm. The distribution is displayed in Fig. 3. The Rh-AgNP's had a zeta potential of +4.3 mV. This gave moderate stability to the biosynthesized nanoparticles due to electrostatic repulsion. Surface charge is an important determinant of nanopar-

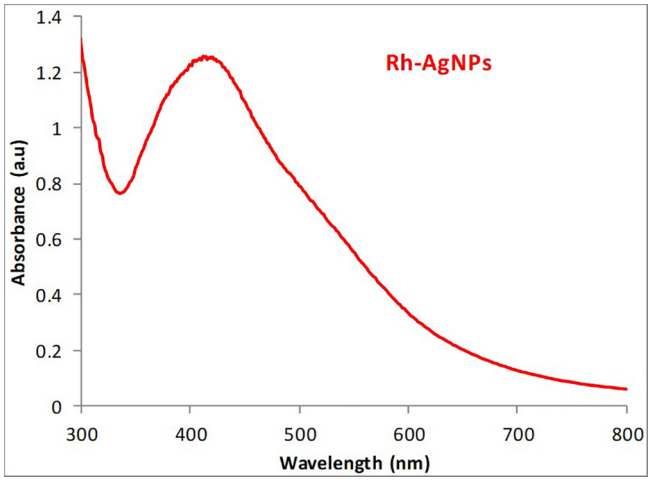

Fig. 2. UV- Vis Spectra of Synthesized Rh-AgNP's.

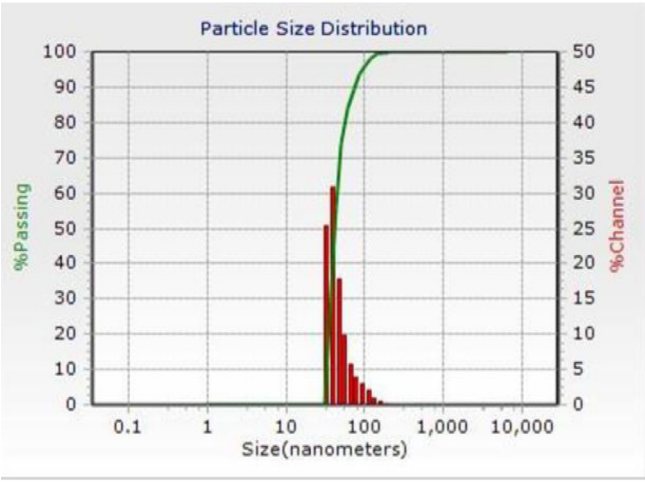

Fig. 3. The hydro dynamic size distribution determined for Rh-AgNP's by dynamic light scattering(DLS); The synthesized Rh-AgNP's analysed for the nanoparticle size distribution.

ticle interactions in biological systems. Chinnappan et al. (2018) have reported similar results for the nanoparticles synthesized by the *Bauhinia purpurea.*

3.2.3. FT-IR spectra of Rh-AgNP's

Fourier Transform Infrared Spectroscopy was used to examine the molecular species present in *R. humilis* and which amongst them participated in stabilization of Rh-AgNP's. The broad peak at 3400 cm^{-1} from the aqueous extract which could be assigned to water O-H group stretch. The Rh-AgNP's spectrum had peaks at 1739 cm^{-1} which attributes to C = 0 stretching frequency, 1638 cm^{-1} which corresponds to C = C alkane chain, 1367 cm^{-1} peak corresponds to CH_3 chain split umbrella mode, 1216 cm^{-1} attributes to C-O-C vibration peaks and 625 cm^{-1} corresponds to the SO_4^{2-} ions which occurs at 580–660 cm^{-1}. (Fig. 4). Reduction of ionic silver and formation of Rh-AgNP's was most probably effected by the aforementioned functional groups arising from the plant extract. while by –OH group stretching broad band at 3349 cm – 1 confirms participation of molecules in *R. humilis* extract. Similar results were reported by the Devaraj et al. (2013); Goswami et al. (2018).

3.2.4. Scanning electron microscope and Energy Dispersive X-ray Spectroscopy

Scanning electron microscopy assessment of Rh-AgNP's nanoparticles size and morphological characteristics at the nanometer to micrometer scale is displayed in Fig. 5B and C. It shows approximate spherical nanoparticles in clusters. Energy Dispersive X-ray Spectroscopy (EDS) spectrum displays the elemental composition of the nanocrystals with presence of an identifiable silver peak. Similar study was reported by Hyllested et al., 2015. larger silver particles may be due to the aggregation of the smaller ones.

3.2.5. Transmission electron microscopic (TEM) for Rh-AgNP's

Transmission electron microscopic (TEM) was used to complement SEM in obtaining the finer details of biosynthesized *R. humilis* silver nanoparticles size and shape (Fig. 5A). The particle had an average sized of 51 nm. findings were similar to other researchers (Singh et al., 2016; Mittal et al., 2013).

3.2.6. X- ray diffraction spectral analysis

X- ray diffraction spectrum of the synthesized silver nanoparticles is given in Fig. 6. The peaks at position 38.07, 44.22, 64.39 and 77.30 in the plot of Intensity count verses 2θ correspond to (1 1 1), (2 0 0), (2 2 0) and (3 1 1) hkl lattice planes of face center cubic (fcc) structure of metallic silver respectively. This confirms that the nanoparticles predominantly were consisted of elemental silver. There were no other conspicuous peaks to signify distinguishable contamination. The results were similar to reports of Anandalakshmi et al. (2016) using Pedalium murex to synthesize silver nanoparticles and Siddiqui et al. (2018) using honey has a reducing agent to synthesis silver nanoparticles.

3.3. DPPH radical scavenging activity of Rh-AgNP's

DPPH activity of silver nanoparticles is measured quantitatively by changes in absorbance (Ajayi & Afolayan, 2017). The dose

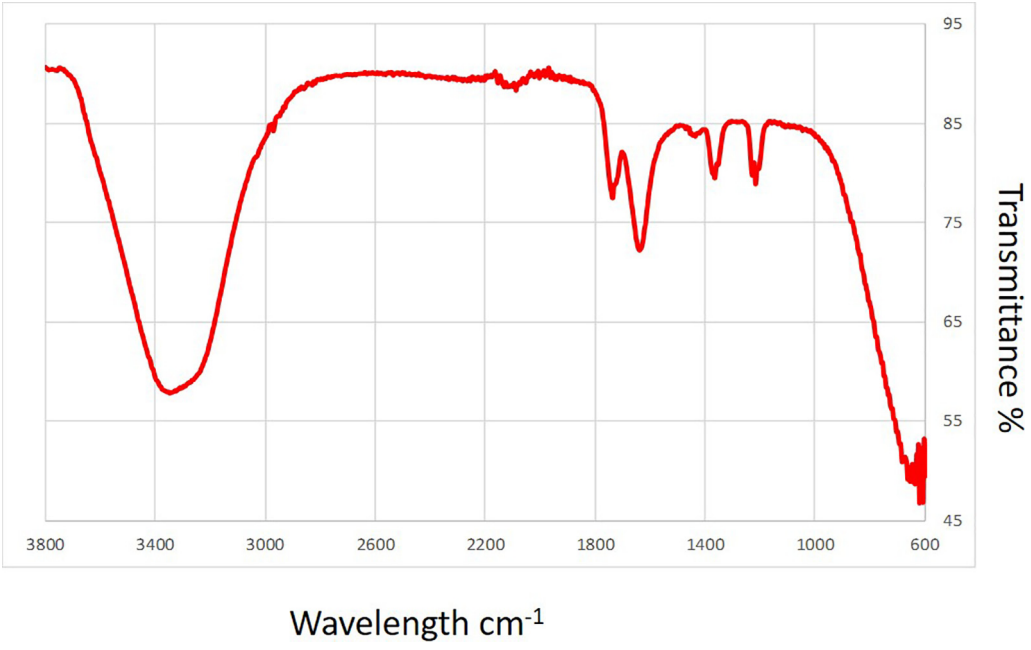

Fig. 4. FT-IR spectra of Rh -AgNP's.

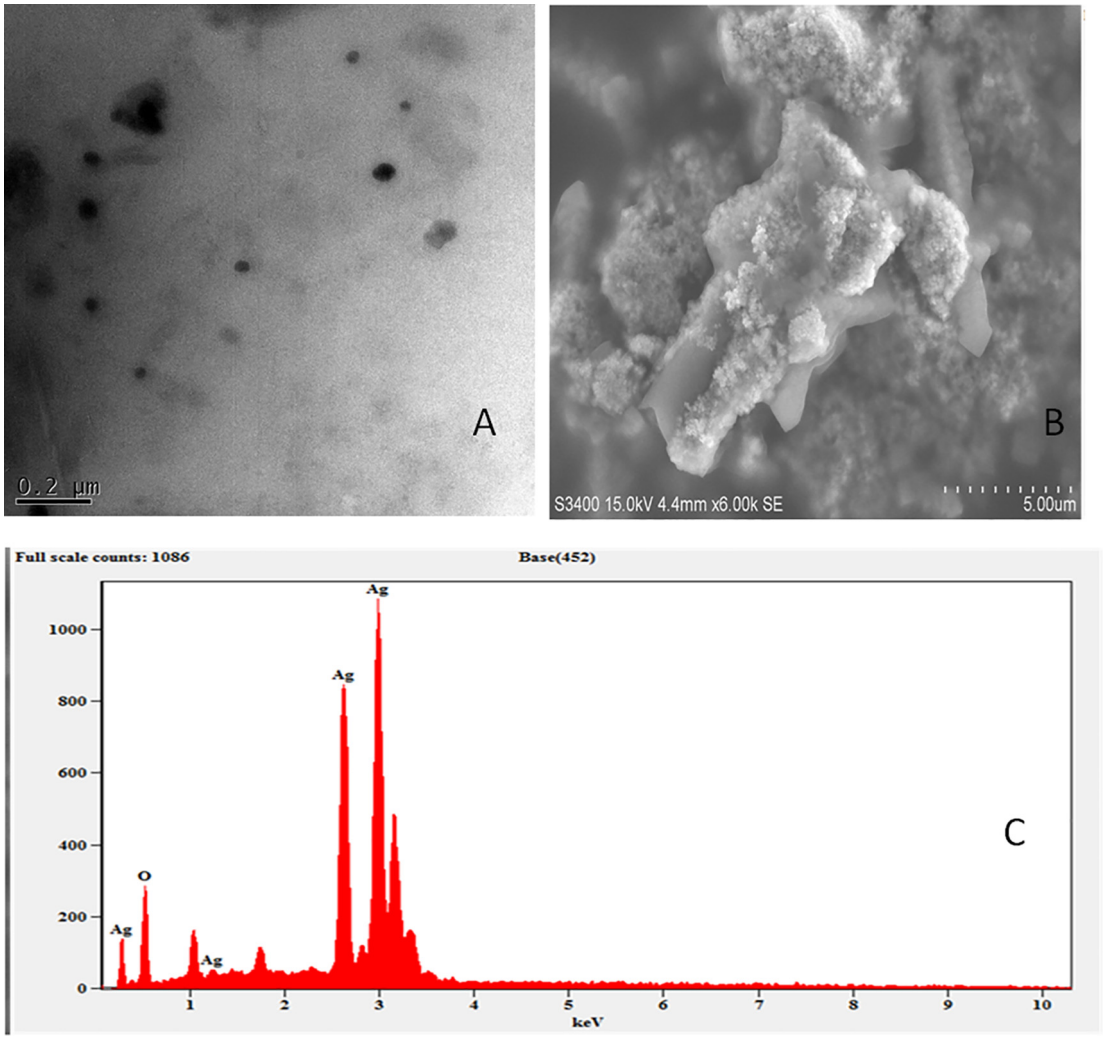

Fig. 5. Transmission Electron Microscopy (A), Scanning Electron Microscopic image (B) and Energy Dispersive X-ray Spectroscopy spectrum (C) of biosynthesized Rh-AgNP's from *R. humilis*. The TEM analysis indicates the spherical shape of the nanoparticles with the average size of 69 nm. The SEM of Rh-AgNP's observed results showed that, the nanoparticles were spherical in shape. The energy dispersive X-ray spectroscopy (EDS) spectrum (B) of Rh-AgNP's showing presence of silver.

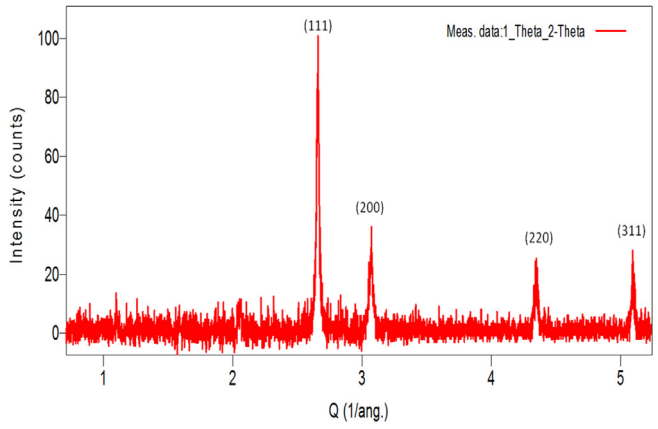

Fig. 6. XRD pattern of Rh-AgNP's- The Synthesized Rh-AgNP's was analysed for crystalline structure of the Rh-AgNP's. The obtained results peak positions were compared with standard. The results showed 2θ peak values at 38.07, 44.22, 64.39 and 77.30 corresponds to (1 1 1), (2 0 0), (2 2 0) and (3 1 1) respectively.

dependent radical scavenging activity significantly elevated with the concentration of Rh-AgNP's (Fig. 7). The experiment was conducted thrice. The significant ($p \leq 0.05$) results was observed in the (Fig. 7). The Scavenging activity of Rh-AgNP's from 0 to 50% with the IC_{50} value of 100 µg/ml compared to standard ascorbic acid which was taken as a control showed RSA of 72% at 50 µg/ml) (Manukumar et al., 2017; Elblbesy, 2016). Earlier reports of Sriranjani et al., 2016; Kharat and Mendhulkar (2016) revealed that plant mediated nanoparticles have enhanced the antioxidant activity.

3.4. Antibrucellosis activity by the Rh-AgNP's

Different dilution concentration of the synthesized Rh-AgNP's were assessed by disc diffusion method and compared with the negative control in dose dependent manner for different *Brucella* cultures. The inhibition zone was observed on the plates and compared with the antibiotics (Fig. 8). The highest antibacterial action exhibited at concentration of 800 ug/mL compared to the standard antibiotic. Similar study was carried out by synthesizing the nanoparticles against *B. melitensis* by Alizadeh et al., 2013.

3.5. Bactericidal effect of Rh- AgNPs on other perilous pathogen

Currently, due to inappropriate use of antibiotics, drug resistant microorganisms are the foremost concern globally. Different con-

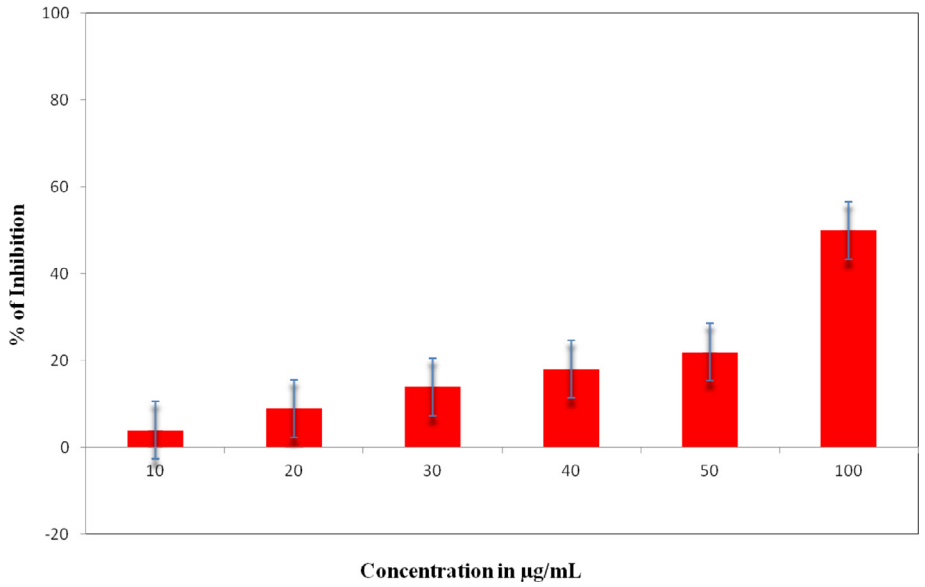

Fig. 7. DPPH radical scavenging activity of Rh-AgNP's; Results show dose dependent radical scavenging property of Rh-AgNP's and exhibited 50% inhibition at the concentration of 100 µg/mL concentration.

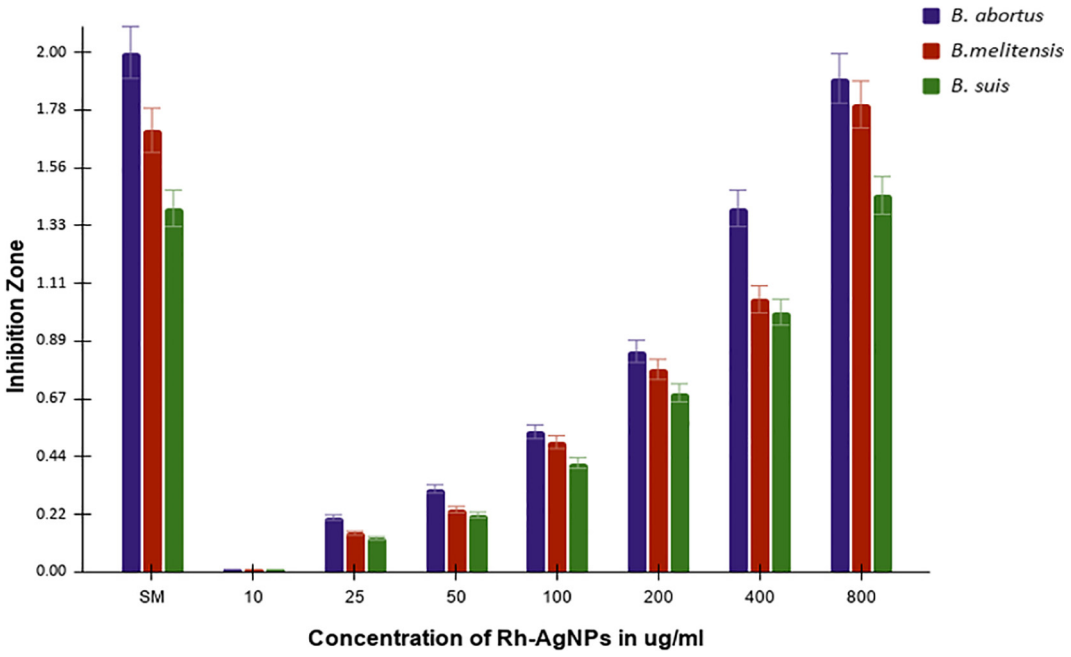

Fig. 8. Antibrucellosis activity by the Rh-AgNP's - Zone of Inhibition from Rh-AgNP's at different concentration 10, 25, 50, 100, 200, 400, 800 µg /mL was tested against *B. abortus, B. melitensis* and *B. suis*, Compared to standard antibiotics SM- Streptomycin. The MIC concentration was found to be 800 µg/mL compared to standard SM (10 µg). All experiments were done in triplicates to assess the veracity of the results.

centration of synthesized Rh-AgNP's was used to assess bactericidal efficacy against different bacteria which resulted in the dose dependent bacterial inhibition. Rh-AgNP exhibited significant inhibition zone against bacteria compared to antibiotics (Table 1). Gram positive *S. aureus* (11 ± 0.1 mm), *B. cereus* (12 ± 0.06 mm), *B. subtilis* (10 ± 0.09 mm) and Gram negative *E. aerogenes* (12 ± 0. 06 mm), *E. coli* (12.50.1 ± mm), *S. flexneri* (13 ± 0.02 mm). Dehghanizade et al., 2018. reported the *Anthemis atropatana* AgNPs showing activity against *S. aureus, S. pyogenes, P. aerugenosa* and *E. coli*. Moodley et al., 2018 reported AgNP's activity against *E. coli, E. facealis, K pneumonia, P. aeruginosa* and *E. coli*. Similar report has been documented by Manukumar et al., 2017; Alfuraydi et al., 2019.

3.6. Biocompatibility assay

3.6.1. Haemolysis assay

The Rh-AgNP's haemolysis activity (<5%) on erythrocytes at different dilutions was evaluated (Fig. 9). Even the small difference in osmolarity and physical change in blood causes their haemolysis resulting in the release of haemoglobin and measured by colorimetric assays. Results indicated that upto 800 µg/mL of Rh-AgNP's can be used for the biological application (Kim and Shin, 2014; Huang et al., 2016). Similarly, Khan et al. (2012) also reported that the *R. humilis* berry juice does not affect the growth and normal biochemical homeostasis hence it is safe to consume without any adverse effect. Selvakumar et al., 2018 have reported

Table 1
Inhibition zone (mm) showing antibacterial activities of the nanoparticles derived from *R. humilis* with the standard drug Streptomycin against bacterial test organisms.

Concentration in μg/ml	25 μg/ml	50 μg/ml	100 μg/ml	200 μg/ml	400 μg/ml	800 μg/ml	1200 μg/ml	SM Std 10 μg
B. cereus	3.4 ± 0.04	4.7 ± 0.04	6 ± 0.02	8.9 ± 0.2	10.5 ± 0.06	11.7 ± 0.1	12 ± 0.06	10 ± 0.2
S. aureus	–	3 ± 0.04	4 ± 0.05	5 ± 0.02	7 ± 0.03	8.5 ± 0.5	11 ± 0.1	12.7 ± 0.09
B. subtilis	–	–	3 ± 0.04	4 ± 0.05	6 ± 0.07	8 ± 0.2	10 ± 0.09	12.2 ± 0.4
E. aeroginosa	3 ± 0.04	4.5 ± 0.04	6 ± 0.02	7 ± 0.06	9.5 ± 0.03	10.8 ± 0.06	12 ± 0.06	12 ± 0.06
S. flexineri	4.6 ± 0.04	6 ± 0.01	7.5 ± 0.03	8.5 ± 0.03	10 ± 0.2	11 ± 0.09	13 ± 0.02	13.4 ± 0.1
E. coli	4 ± 0.04	5 ± 0.05	7.5 ± 0.04	8.4 ± 0.03	9.5 ± 0.2	10.5 ± 0.06	12.5 ± 0.1	11.8 ± 0.06

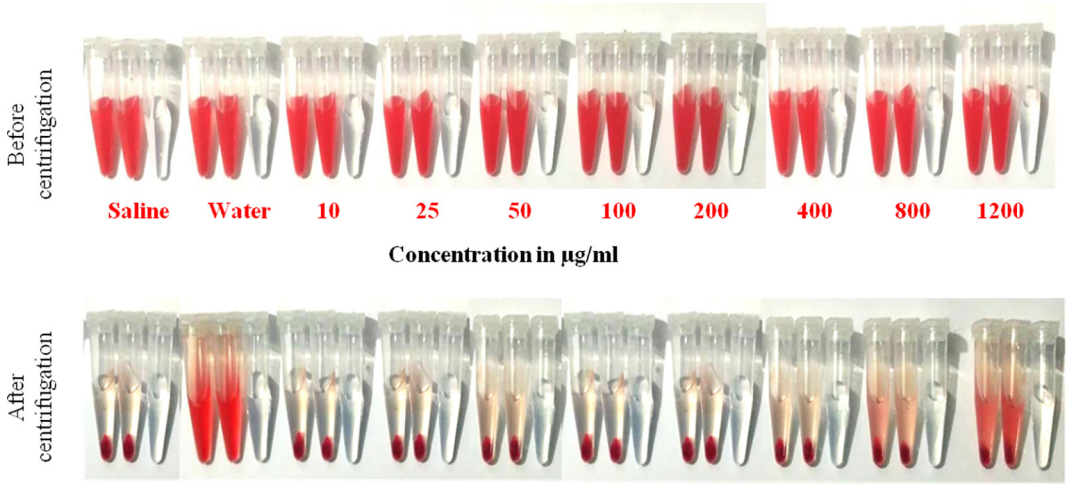

Fig. 9. The biocompatibility on RBCs. The Rh-AgNP's samples treated with citrated blood for different concentrations. Rh-AgNP's did not show any effect up to 400 ug/mL, but 800 ug onwards shows a significant effect on RBCs to cause haemolysis. Before and after centrifugation shows an effect of Rh-AgNP's for haemolysis, saline and distilled water used as a negative and positive control.

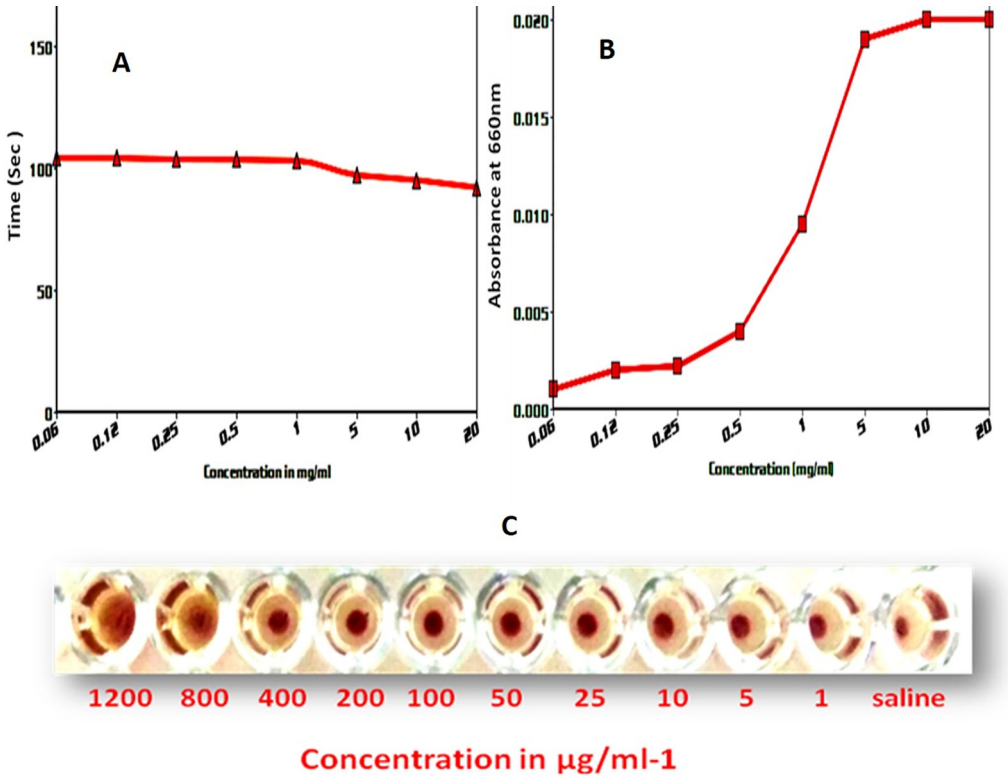

Fig. 10. Fibrinolytic and hemagglutination assay- The lysis of fibrin clot and clotting time of citrated plasma at various concentrations of Rh-AgNP's is depicted in (A and B) the hemagglutination assay(C) depicted that the agglutination of red blood cells by Rh-AgNP's.

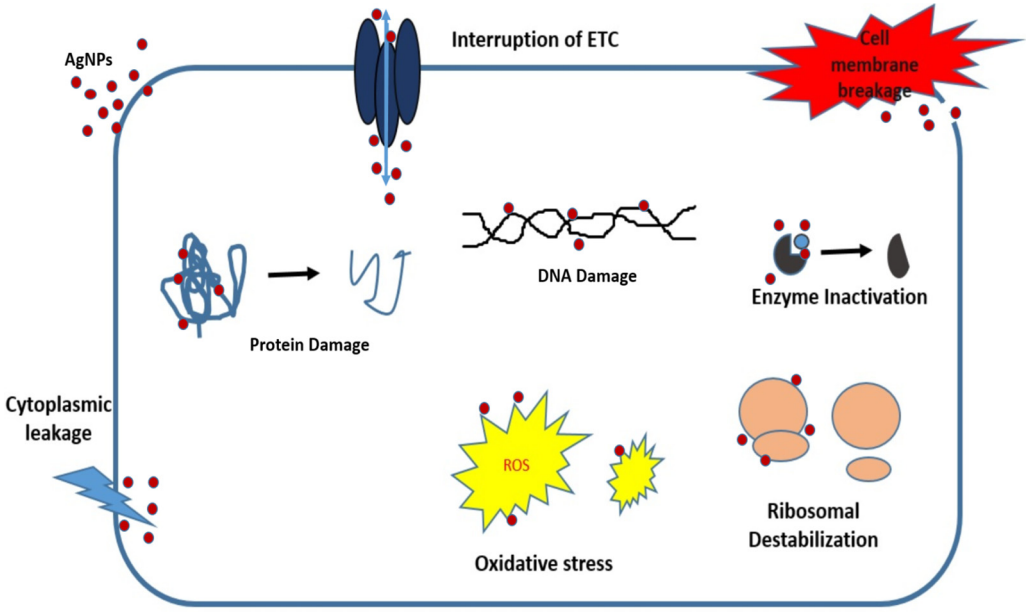

Fig. 11. Plausible molecular mechanism of the Green synthesized silver nanoparticles against bacteria.

that AgNPs of *Acalypha hispida* have similar biocompatibility activity.

3.6.2. Fibrinolytic assay

Rh-AgNP's depicted plasmin-like activity by considerable fibrin clot hydrolysis in a dose-dependent manner (Fig. 10A). Stability of nanoparticles is very significant to for the biological application. Rh-AgNP's in the presence of chelator EDTA and EGTA did not show any defect in blood coagulation and rate of re-clarification of citrated plasma (Fig. 10B) (Lateef et al., 2016).

3.6.3. Hemagglutination assay

Hemagglutination assay revealed that the Rh-AgNP's at a concentration of 1200 and 800 μg/mL agglutinated the RBC cells (Fig. 10(C)). Below 400 μg/ml dilutions did not show agglutinating activity. It increases efficacy of silver nanoparticles applications in biological domain. From the present study we can say that, the Rh-AgNP's are biocompatible with the red blood cells. Similar results were observed for Capsaicin-capped silver nanoparticles by Amruthraj et al., 2015. Hence, the Rh-AgNP's can be used has a potential drug after the invivo studies. Based on the above observation the plausible molecular action of green synthesized silver nanoparticle against bacteria (Fig. 11).

4. Conclusion

The silver nanoparticles synthesized by *R. humilis* is cost effective, efficient and environmental friendly process. Morphologically distinct silver nanoparticles synthesized were characterized. Formation of bio-functionalized spherical AgNP's with a size mean of 51 nm was confirmed using UV–VIS, FTIR, SEM, EDS, and TEM. XRD and DLS, Zeta potential confirms the stability of the formed AgNPs. Rh-AgNP's showed a dose-dependent radical scavenging activity. Antibacterial results show that the Rh-AgNP's were inhibiting the growth of *Brucella* species. The biocompatibility of synthesized Rh-AgNP's by rate of haemolysis, Fibrinolytic activity and Hemagglutination assay showed the efficacy of synthesized Rh-AgNP's in the biological domain. This study revealed that the Rh-AgNP's can be used in biological application.

Declaration of Competing Interest

The authors declare that they have no known competing financial interests or personal relationships that could have appeared to influence the work reported in this paper.

Acknowledgments

The authors Sri Raghava and Umesha, S. greatly acknowledge the financial assistance from the ICMR in the form of Research associate (No. Fellowship/28/2018/ECD-II), Government of India, New Delhi, India. We also thank Institution of Excellence at University of Mysore for providing instrumentation facility.

References

Aboaba, O.O., Smith, S.I., Olude, F.O., 2006. Antibacterial effect of edible plant extract on Escherichia coli 0157: H7. Pakistan J. Nutr. 5, 325–327.
Ajayi, E., Afolayan, A., 2017. Green synthesis, characterization and biological activities of silver nanoparticles from alkalinized Cymbopogon citratus Stapf. Adv. Natl. Sci.: Nanosci. Nanotechnol. 8, 015017.
Alfuraydi, A.A., Devanesan, S., Al-Ansari, M., AlSalhi, M.S., Ranjitsingh, A.J., 2019. Eco-friendly green synthesis of silver nanoparticles from the sesame oil cake and its potential anticancer and antimicrobial activities. J. Photochem. Photobiol., B 192, 83–89.
Alizadeh, H., Salouti, M., Shapouri, R., 2013. Intramacrophage antimicrobial effect of silver nanoparticles against Brucella melitensis 16M. Sci. Iran 20, 1035–1038.
Amruthraj, N.J., Raj, J.P.P., Lebel, A., 2015. Capsaicin-capped silver nanoparticles: its kinetics, characterization and biocompatibility assay. Appl. Nanosci. 5, 403–409.
Anandalakshmi, K., Venugobal, J., Ramasamy, V., 2016. Characterization of silver nanoparticles by green synthesis method using Pedalium murex leaf extract and their antibacterial activity. Appl. Nanosci. 6, 399–408.
Bastús, N.G., Piella, J., Puntes, V., 2015. Quantifying the sensitivity of multipolar (dipolar, quadrupolar, and octapolar) surface plasmon resonances in silver nanoparticles: the effect of size, composition, and surface coating. Langmuir 32, 290–300.
Brahmachari, G., Sarkar, S., Ghosh, R., Barman, S., Mandal, N.C., Jash, S.K., Banerjee, B., Roy, R., 2014. Sunlight-induced rapid and efficient biogenic synthesis of silver nanoparticles using aqueous leaf extract of Ocimum sanctum Linn. with enhanced antibacterial activity. Org. Med. Chem. Lett. 4, 18.
Chinnappan, S., Kandasamy, S., Arumugam, S., Seralathan, K.K., Thangaswamy, S., Muthusamy, G., 2018. Biomimetic synthesis of silver nanoparticles using flower extract of Bauhinia purpurea and its antibacterial activity against clinical pathogens. Environ. Sci. Pollut. Res. 25, 963–969.

Dehghanizade, S., Arasteh, J., Mirzaie, A., 2018. Green synthesis of silver nanoparticles using Anthemis atropatana extract: characterization and in vitro biological activities. Artif. Cells Nanomed. Biotechnol. 46, 160–168.
Devaraj, P., Kumari, P., Aarti, C., Renganathan, A., 2013. Synthesis and characterization of silver nanoparticles using cannonball leaves and their cytotoxic activity against MCF-7 cell line. J. Nanotechnol. 2013.
Elblbesy, M.A., 2016. Hemocompatibility of albumin nanoparticles as a drug delivery system—an in vitro study. J. Biomater. Nanobiotechnol. 7, 64.
Ghaderkhani, J., Yousefimashouf, R., Arabestani, M., Roshanaei, G., Asl, S.S., Abbasalipourkabir, R., 2019. Improved antibacterial function of Rifampicin-loaded solid lipid nanoparticles on Brucella abortus. Artif. Cells Nanomed. Biotechnol. 47, 1181–1193.
Ghanwate, N., Thakare, P., Bhise, P.R., Gawande, S., 2016. Colorimetric method for rapid detection of Oxacillin resistance in Staphylococcus aureus and its comparison with PCR for mec A gene. Sci. Rep. 6, 23013.
Goswami, M., Baruah, D., Das, A.M., 2018. Green synthesis of silver nanoparticles supported on cellulose and their catalytic application in the scavenging of organic dyes. New J. Chem. 42, 10868–10878.
Grilló, M.J., Manterola, L., De Miguel, M.J., Muñoz, P.M., Blasco, J.M., Moriyón, I., López-Goñi, I., 2006. Increases of efficacy as vaccine against Brucella abortus infection in mice by simultaneous inoculation with avirulent smooth bvrS/bvrR and rough wbkA mutants. Vaccine 24, 2910–2916.
Hamedi, S., GhaseFminezhad, M., Shokrollahzadeh, S., Shojaosadati, S.A., 2017. Controlled biosynthesis of silver nanoparticles using nitrate reductase enzyme induction of filamentous fungus and their antibacterial evaluation. Artif. Cells Nanomed. Biotechnol. 45, 1588–1596.
Harish, B.S., Uppuluri, K.B., Anbazhagan, V., 2015. Synthesis of fibrinolytic active silver nanoparticle using wheat bran xylan as a reducing and stabilizing agent. Carbohydr. Polym. 132, 104–110.
Harsha, P.S.C., Khan, M.I., Giridhar, P., Ravishankar, G.A., 2012. In vitro propagation of Rivina humilis L. through proliferation of axillary shoots and shoot tips of mature plants.
Huang, H., Lai, W., Cui, M., Liang, L., Lin, Y., Fang, Q., Liu, Y., Xie, L., 2016. An evaluation of blood compatibility of silver nanoparticles. Sci. Rep. 6, 25518.
Hyllested, J.Æ., Palanco, M.E., Hagen, N., Mogensen, K.B., Kneipp, K., 2015. Green preparation and spectroscopic characterization of plasmonic silver nanoparticles using fruits as reducing agents. Beilstein J. Nanotechnol. 6, 293–299.
Jayapriya, M., Dhanasekaran, D., Arulmozhi, M., Nandhakumar, E., Senthilkumar, N., Sureshkumar, K., 2019. Green synthesis of silver nanoparticles using Piper longum catkin extract irradiated by sunlight: antibacterial and catalytic activity. Res. Chem. Intermediat. 45, 3617–3631.
Khan, M.I., Harsha, P.S., Giridhar, P.S.C.P., Ravishankar, G.A., 2012. Pigment identification, nutritional composition, bioactivity, and in vitro cancer cell cytotoxicity of Rivina humilis L. berries, potential source of betalains. LWT 47, 315–323.
Kharat, S.N., Mendhulkar, V.D., 2016. Synthesis, characterization and studies on antioxidant activity of silver nanoparticles using Elephantopus scaber leaf extract. Mater. Sci. Eng., C 62, 719–724.
Kim, M.J., Shin, S., 2014. Toxic effects of silver nanoparticles and nanowires on erythrocyte rheology. Food Chem. Toxicol. 67, 80–86.
Kirk, M.D., Pires, S.M., Black, R.E., Caipo, M., Crump, J.A., Devleesschauwer, B., Döpfer, D., Fazil, A., Fischer-Walker, C.L., Hald, T., Hall, A.J., 2015. World Health Organization estimates of the global and regional disease burden of 22 foodborne bacterial, protozoal, and viral diseases, 2010: a data synthesis. PLoS Med. 12, 1001921.
Lateef, A., Akande, M.A., Ojo, S.A., Folarin, B.I., Gueguim-Kana, E.B., Beukes, L.S., 2016. Paper wasp nest-mediated biosynthesis of silver nanoparticles for antimicrobial, catalytic, anticoagulant, and thrombolytic applications. 3 Biotech. 6, 140.
Manukumar, H.M., Umesha, S., Kumar, H.N., 2017. Promising biocidal activity of thymol loaded chitosan silver nanoparticles (TC@ AgNPs) as anti-infective agents against perilous pathogens. Int. J. Biol. Macromol. 102, 1257–1265.
Mittal, A.K., Chisti, Y., Banerjee, U.C., 2013. Synthesis of metallic nanoparticles using plant extracts. Biotechnol. Adv. 31, 346–356.
Moodley, J.S., Krishna, S.B.N., Pillay, K., Govender, P., 2018. Green synthesis of silver nanoparticles from Moringa oleifera leaf extracts and its antimicrobial potential. Adv. Natl. Sci. J. Nanosci. Nanotechnol. 1, 015011.
Muthuraman, M.S., Nithya, S., Christena, L.R., Vadivel, V., Subramanian, N.S., Anthony, S.P., 2019. Green synthesis of silver nanoparticles using Nardostachys jatamansi and evaluation of its anti-biofilm effect against classical colonizers. Microb. Pathog. 126, 1–5.
Odeyemi, S., Afolayan, A., Bradley, G., 2015. In vitro anti-inflammatory and free radical scavenging activities of crude saponins extracted from Albuca bracteata Jacq. Bulb. Afr. J. Tradit. Complement. Altern. Med. 12, 34–40.
Pishahang, J., Amiri, H.B., Heli, H., 2018. Synthesis of carbon nanoparticles-poly (ortho-aminophenol) nanocomposite and its application for electroanalysis of iodate. Sens. Actuators B: Chem. 256, 878–887.
Raghava, S., Honnayakanahalli, M.G.M., Shome, R., Kulkarni, M., Umesha, S., 2017. Epidemiological and molecular characterization of Brucella species in cattle. Asian J. Anim. Sci. 11, 123–131.
Rastogi, L., Arunachalam, J., 2011. Sunlight based irradiation strategy for rapid green synthesis of highly stable silver nanoparticles using aqueous garlic (Allium sativum) extract and their antibacterial potential. Mater. Chem. Phys. 129, 558–563.
Selvakumar, P., Sithara, R., Viveka, K., Sivashanmugam, P., 2018. Green synthesis of silver nanoparticles using leaf extract of Acalypha hispida and its application in blood compatibility. J. Photochem. Photobiol., B 182, 52–61.
Selvan, D.A., Mahendiran, D., Kumar, R.S., Rahiman, A.K., 2018. Garlic, green tea and turmeric extracts-mediated green synthesis of silver nanoparticles: phytochemical, antioxidant and in vitro cytotoxicity studies. J. Photochem. Photobiol., B 180, 243–252.
Siddiqui, M.N., Redhwi, H.H., Achilias, D.S., Kosmidou, E., Vakalopoulou, E., Ioannidou, M.D., 2018. Green synthesis of silver nanoparticles and study of their antimicrobial properties. J. Polym. Environ. 26, 423–433.
Singh, P.K., Sah, P., Meher, J.G., Joshi, S., Pawar, V.K., Raval, K., Singh, Y., Sharma, K., Kumar, A., Dube, A., Chourasia, M.K., 2016. Macrophage-targeted chitosan anchored PLGA nanoparticles bearing doxorubicin and amphotericin B against visceral leishmaniasis. RSC Adv. 6, 71705–71718.
Soshnikova, V., Kim, Y.J., Singh, P., Huo, Y., Markus, J., Ahn, S., Castro-Aceituno, V., Kang, J., Chokkalingam, M., Mathiyalagan, R., Yang, D.C., 2018. Cardamom fruits as a green resource for facile synthesis of gold and silver nanoparticles and their biological applications. Artif. Cells Nanomed. Biotechnol. 46, 108–117.
Sriranjani, R., Srinithya, B., Vellingiri, V., Brindha, P., Anthony, S.P., Sivasubramanian, A., Muthuraman, M.S., 2016. Silver nanoparticle synthesis using Clerodendrum phlomidis leaf extract and preliminary investigation of its antioxidant and anticancer activities. J. Mol. Liq. 220, 926–930.
Thangaraju, N., Venkatalakshmi, R.P., Chinnasamy, A., Kannaiyan, P., 2012. Synthesis of silver nanoparticles and the antibacterial and anticancer activities of the crude extract of Sargassum polycystum C. Arghad Nano Biomed. Eng. 4, 89–94.
Tseng, Y.H., Wang, C.C., Chen, Y.T., 2008. Rivina humilis L. (Phytolaccaceae), a newly naturalized plant in Taiwan. Taiwania 53, 417–419.
Vilchis-Nestor, A.R., Sánchez-Mendieta, V., Camacho-López, M.A., Gómez-Espinosa, R.M., Camacho-López, M.A., Arenas-Alatorre, J.A., 2008. Solventless synthesis and optical properties of Au and Ag nanoparticles using Camellia sinensis extract. Mater. Lett. 62, 3103–3105.
Werka, J.S., Boehme, A.K., Setzer, W.N., 2007. Biological activities of essential oils from Monteverde, Costa Rica. Nat. Prod. Commun. 2. 1934578X0700201204.